The role of static disorder in negative thermal expansion in ReO_3

Efrain E. Rodriguez,[1,2] Anna Llobet,[1] Thomas Proffen,[1] Brent C. Melot,[2]
Ram Seshadri,[2] Peter B. Littlewood,[3] and Anthony K. Cheetham[4,*]

[1]*Los Alamos National Laboratory, Lujan Neutron Scattering Center, MS H805, Los Alamos, NM 87545, USA*
[2]*Materials Department and Materials Research Laboratory, University of California, Santa Barbara, CA 93106, USA*
[3]*Cavendish Laboratory, University of Cambridge, Madingley Road, Cambridge, CB3 OHE, UK*
[4]*Department of Materials Science and Metallurgy, University of Cambridge, Pembroke Street, Cambridge, CB2 3QZ, UK*

Time-of-flight neutron powder diffraction and specific heat measurements were used to study the nature of thermal expansion in rhenium trioxide, an electrically conducting oxide with cubic symmetry. The temperature evolution of the lattice parameters show that ReO_3 can exhibit negative thermal expansion at low temperatures and that the transition from negative to positive thermal expansion depends on sample preparation; the single crystal sample demonstrated the highest transition temperature, 300 K, and largest negative value for the coefficient of thermal expansion, $\alpha = -1.1(1) \times 10^{-6}$ K $^{-1}$. For the oxygen atoms, the atomic displacement parameters are strongly anisotropic even at 15 K, indicative of a large contribution of static disorder to the displacement parameters. Further inspection of the temperature evolution of the oxygen displacement parameters for different samples reveals that the static disorder contribution is greater for the samples with diminished NTE behavior. In addition, specific heat measurements show that ReO_3 lacks the low energy Einstein-type modes seen in other negative thermal expansion oxides such as ZrW_2O_8.

I. INTRODUCTION

Metals that contract upon heating are exceedingly rare, if they exist at all. This observation can be understood by considering the types of cohesive interactions bonding atoms into solids. As a material is heated, interatomic distances expand due to the asymmetric shape of the potential energy well and therefore to anharmonic effects.[1, 2] A chemical bond with a deeper potential well will confine atomic vibrations to remain more harmonic and consequently, covalently bonded materials such as diamond exhibit lower thermal expansion than metals such as copper. In some covalent crystals with open framework structures, the low thermal expansion can even become negative. Among the negative thermal expansion (NTE) materials most studied are framework oxides such as ZrW_2O_8[3, 4, 5] and more recently metal cyanide frameworks such as $Zn(CN)_2$,[6, 7] all of which are electrical insulators or semiconductors. In contrast, the oxide ReO_3 is a superb electrical conductor with a room temperature resistivity close to that of copper.[8, 9] Recently, Chatterji *et al.* have demonstrated through neutron powder diffraction and first-principles calculations that ReO_3 also exhibits isotropic NTE,[10] making it the only known simple binary oxide to combine metallic conductivity with NTE.

A topological feature that can lead to NTE behavior in an open framework structure is a linear chain consisting of a ligand coordinated to two metals or *vice versa*.[2, 11] For example, simple binary oxides such as Cu_2O, Ag_2O (O–M–O chains)[12]and certain phases of SiO_2 (Si–O–Si chains)[13, 14] demonstrate NTE behavior. While this is not a requisite for NTE behavior (magnetostriction and phase transitions can also result in NTE), it is a simple principle by which new NTE materials can be pursued. The structure of rhenium trioxide contains such linear chains in a three dimensional framework consisting of corner-sharing ReO_6 octahedra (See Fig. 1). The

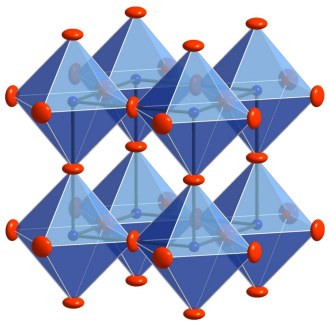

FIG. 1: The crystal structure of the cubic perovskite ReO_3. ReO_6 octahedra connect via corner-sharing in infinite chains in all three directions. The atomic displacement ellipsoids of the oxygen atoms (in red) are represented at 90 % probability; their flat shape indicates transverse displacement normal to the Re–O–Re bonds and into the void in the middle of the cubic cell.

*Electronic address: akc30@cam.uc.uk

simple ReO_3 structure is a prototype for closely related materials such as the perovskite ferroelectrics, ferromagnets, and high T_c superconductors and can also be thought of as the cubic perovskite ABO_3 with a void in the place of the A cation.

Thermal expansion investigations of ReO_3 have presented conflicting results. A laser interferometry study on a single crystal concluded that ReO_3 displayed NTE between 100 K and 340 K,[15]. In contrast to the single crystal work, a catalogue of powder X-ray diffraction (XRD) studies reported the coefficient of thermal expansion of ReO_3 to be small but positive for all temperature ranges.[16] The latter study has been more frequently cited in reviews of NTE in oxide frameworks,[2, 17] leaving ReO_3 largely unrecognized as a potential NTE material until the recent article by Chatterji *et al*, which showed through diffraction studies NTE up to 200 K.[10] In the present study, we show that ReO_3 can exhibit isotropic NTE up to room temperature, that the positive to negative transition is dependent on sample quality, and that specific heat measurements show a lack of any low energy Einstein-type modes that lead to the NTE behavior in other oxides. Furthermore, we show through careful analysis of the atomic displacement parameters the role of static disorder of the oxygen atoms in impeding NTE behavior and therefore explain the discrepancy between past thermal expansion studies of ReO_3.

II. EXPERIMENTAL METHODS

The thermal expansion properties of various ReO_3 powder samples were investigated by performing variable temperature neutron powder diffraction (NPD) with time-of-flight neutron data. The first sample investigated, labeled ReO_3-a throughout this paper, was a powder prepared by the decomposition of an Re_2O_7–1,4 dioxane adduct at 140 °C as first described by Nechamkin *et al.*[18] The second sample studied, ReO_3-b, was a powder purchased from Alfa Aesar (99.99% chemical purity). Finally, the third sample, ReO_3-c, was prepared by crushing single crystals of ReO_3 grown by chemical vapor transport (CVT). By using $HgCl_2$ as the transport agent in an evacuated Pyrex glass ampoule with ReO_3 powder (ReO_3-b as the starting powder), the crystals were grown across a temperature gradient of about 100 °C as described by Feller *et al.*[19]. In addition to growing single crystals, CVT also separates the lower oxide phase impurities from the freshly grown ReO_3 crystals. Hence, sample ReO_3-c was expected to be of higher chemical and phase purity than the others.

NPD patterns were obtained on the high intensity powder diffractometer (HIPD) at the Lujan Neutron Scattering Center at the Los Alamos Neutron Science Center (LANSCE). HIPD is suitable for studying the behavior of materials as a function of temperature and pressure due to its relatively high data acquisition rates. HIPD data were collected on all samples between 15 K and 300 K. The Lujan Center employs a pulsed spallation neutron source, so the NPD histograms were collected in time-of-flight mode on fixed detector banks. The backscattering detector banks, located ±153° with respect to the incident beam, provide the highest resolution pattern and higher-index reflections while the normal (±90°) and forward scattering (±40°) banks have a lower resolution but probe higher d-spacings. In the study by Chatterji *et al.*, the neutron diffraction measurements were performed on a constant wavelength source ($\lambda = 1.359 \pm 0.001$ Å),[10] limiting the diffractogram up to 8.5 $Å^{-1}$ in momentum transfer $Q = 4\pi \sin\theta/\lambda$. More accurate structural parameters such as atomic displacement parameters can be accessed with time-of-flight neutron data since higher Q ranges can be probed. In our measurements, a Q_{max} of 16 $Å^{-1}$ was used for all the structural refinements.

The specific heat data were collected upon warming from 2 K to 20 K on a 28.5 mg single crystal using a quasiadiabatic method as implemented on a Quantum Design Physical Property Measurement System (PPMS). Like sample ReO_3-c, the single crystal was grown by CVT.

III. RESULTS AND DISCUSSION

Least squares structural refinements by the Rietveld method were performed with all six histograms of the NPD data using the GSAS software package.[20] In space group $Pm\bar{3}m$, only four variables were refined for each temperature: the lattice parameter; the isotropic displacement parameter U_{iso} of Re, and the anisotropic displacement parameters U_{11} (= U_{22}), and U_{33} of O. To determine the lattice parameters of the sample accurately, X-ray powder diffraction was performed at room temperature with Si Standard Reference Material 640c purchased from National Institute of Standards (See Fig. 2a). The neutron powder profile for the sample prepared from single crystals, ReO_3-c, is shown in Fig. 2b. In this sample, the lattice parameter plotted as a function of temperature clearly demonstrates NTE behavior from 15 K up to 300 K (See Fig. 3c). NTE in the other powder samples was indeed observed but limited to a narrower temperature range (See Fig. 3a,b). For sample ReO_3-a, the NTE behavior was observed only up to 110 K, and for ReO_3-b,

only up to 220 K. Clearly sample quality has an effect on the thermal expansion properties and this may, in part, explain the discrepancy between past findings on the thermal expansion behavior of ReO_3 and the reason why Chatterji *et al.* found NTE only up to 200 K from their neutron measurements while their dynamical lattice calculations predicted NTE up to 350 K.[10]

The linear coefficient of thermal expansion for a cubic system α is defined as $\alpha = (1/a) \times \partial a/\partial T$ where a is the cubic cell parameter and T the temperature. A least squares polynomial fit (second-order) to the lattice parameters obtained from the neutron data affords $a(T)$, which can be differentiated with respect to T and divided by the experimental values of a to obtain α as a function of T. For sample ReO_3-c the average α below 300 K was found to be $-1.1(1) \times 10^{-6}\,K^{-1}$. For sample ReO_3-a, α was found to be $-3.5(6) \times 10^{-7}\,K^{-1}$, and $-6.4(5) \times 10^{-7}\,K^{-1}$ for sample ReO_3-b. Thus, lowering of the transition temperature $T_{NTE \rightarrow PTE}$ is correlated with a smaller, negative value for α.

For sample ReO_3-c, the values for $\alpha(T)$ are close to those determined by Matsuno *et al.* in their interferometry study on single crystals where the value of α is $-2 \times 10^{-6}\,K^{-1}$ at about 120 K and slowly rises to $-1 \times 10^{-6}\,K^{-1}$ at about 230 K.[15] While we did not make measurements above room temperature, Matsuno *et al.* found α to be positive and smaller than $2 \times 10^{-6}\,K^{-1}$ between 340 K and 500 K.[15] In an XRD study carried out on single crystals as well as powder samples, Chang *et al.* found a value of $1.1(1) \times 10^{-6}\,K^{-1}$ above room temperature.[21] The volumetric α calculated by Chatterji *et al.* is not linear as in our simplified model from the fitted curves, but nevertheless shows a volumetric α (= 1/3 linear α) varying between -2×10^{-6} to zero below 350 K.[10]

The atomic displacement parameters obtained from the NPD data offer some clues as to the mechanism responsible for NTE in ReO_3. Due to the high range of momentum transfer Q available from time-of-flight neutrons as well as the lack of any decay with Q in the atomic form factors for neutron

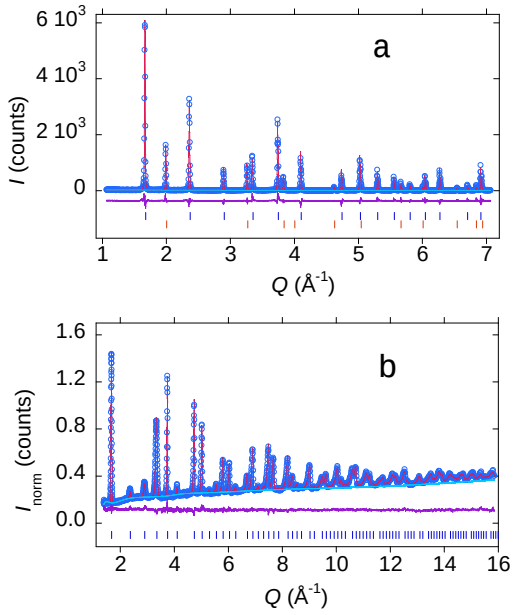

FIG. 2: (a) Observed profile of ReO_3 from X-rays shown in open circles and the calculated profile as a smooth red line. The X-ray powder patterns contain both sample ReO_3-c and a Si standard. Upper tickmarks correspond to ReO3-c and lower to the Si standard. (b) Observed profile from neutrons is shown in open circles and the calculated as a smooth red line for sample ReO_3-c only with corresponding Bragg reflection tickmarks below. The difference curve between the observed and calculated patterns are represented by the smooth purple line below the powder profiles.

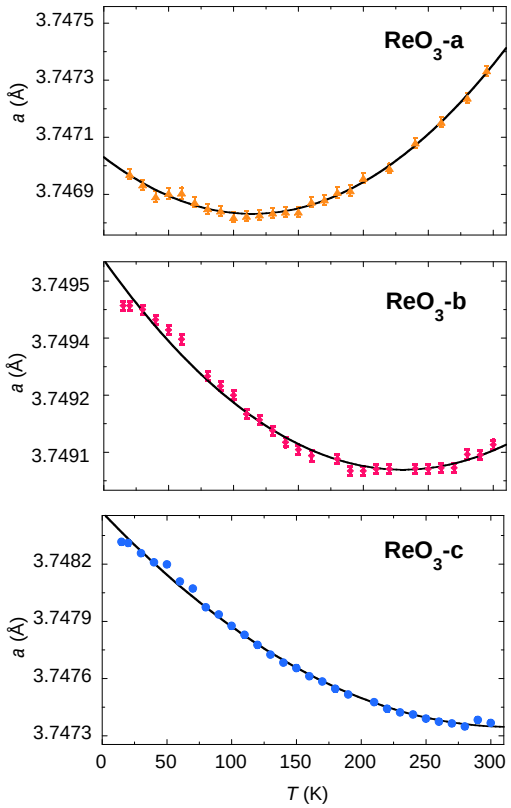

FIG. 3: Temperature evolution of the lattice parameters obtained from neutron diffraction for samples ReO_3-a, ReO_3-b, and ReO_3-c. The smooth black curves are the least-squares, polynomial fits to the lattice parameters. Error bars are obtained from standard uncertainties in the structural refinements.

diffraction, accurate atomic displacement parameters were obtained from the Rietveld analysis (See Fig. 4a). The Re atom is located on the special position $1a$ (site symmetry $\bar{3}m$), which constrains the atomic displacement parameter to remain isotropic. The oxygen atoms are located on the position $3c$ (site symmetry $4/mmm$), constraining them to have only two values, U_{11} $(= U_{22})$ and U_{33}. While the displacement of the O atoms along the Re–O–Re direction remains fairly constant, the transverse motion increases upon heating, as also observed by Chatterji *et al.*[10] The most striking feature is the gap between U_{11} $(= U_{22})$ and U_{33} as represented by the flatness of the displacement ellipsoids of the O atoms (See Fig. 1). The anisotropy only increases with temperature, suggesting that the transverse motion contracts the cubic lattice upon heating and is therefore the most likely mechanism for the observed NTE behavior.

Further inspection of the oyxgen displacement parameters of all three samples reveals differences that may explain the varying thermal expansion behavior. Though sometimes loosely referred to as thermal parameters or Debye-Waller factors, the values for U_{ij} have contributions from both dynamic and static displacements of the atoms. Extrapolation of the U_{ij} parameters for ReO_3 down to 0 K reveals non-zero values, which indicates significant contribution from static displacement, especially in the case of U_{11} (See Fig. 4a). The large gap between U_{11} and U_{33} at low temperatures was observed for all three samples. A useful parameter to describe the extent of anisotropy in the atomic displacements is the ratio of the maximum value to the minimum value of U_{ij};[22] in our case, it is U_{11}/U_{33}. When plotted versus temperature (See Fig. 4b,c), this measure of anisotropy reveals that it is constant (within the error bars) and large for sample ReO_3-a, while it is increases upon heating for ReO_3-b and ReO_3-c. Most importantly, the higher U_{11}/U_{33} ratios for ReO_3-a and ReO_3-b than for ReO_3-c at low temperatures suggest more static disorder in the first two, which should affect the lattice dynamical properties. The $M3$ mode calculated by Chatterji *et al* involves rotation of the ReO_6 octahedra in the $a-b$ plane and arises from transverse motion of the O atoms in this plane.[10] Since the $M3$ mode has the largest contribution to the negative value for α at low temperatures, static displacement of the O atoms, transversely from the Re–O–Re bond, would diminish the NTE behavior.

Specific heat measurements on a single crystal of ReO_3 were carried out to understand the type of lattice vibrations contributing to the specific heat. The low temperature behavior in the heat capacity of ReO_3 is that of a straightforward Debye solid, with a Debye temperature Θ of 344 K and a Sommerfeld coefficient γ of 2.8 mJ mol^{-1} K^{-2} (See Fig. 5a). These values agree very well with the values of 327 K for Θ and 2.85 mJ mol^{-1} K^{-2} for γ found in the early studies by King *et al.*[9] Fig. 5b shows the specific heat over T^3 vs. $\ln T$, which is an approximate representation of the one-dimensional phonon density of states of a solid.[23, 24] A signature of an Einstein mode in this representation is a Gaussian-like peak–clearly missing in the low temperature region of the specific heat. These measurements strengthen the argument by Chatterji *et al.* from their lattice dynamical calculations that NTE in ReO_3 is caused by low energy acoustic modes with the $M3$ mode contributing the most to the NTE behavior.[10] Also, the specific heat results rule out the suggestion by Matsuno *et al.* that a low energy, bending-like optical mode is responsible for NTE in ReO_3.[15]

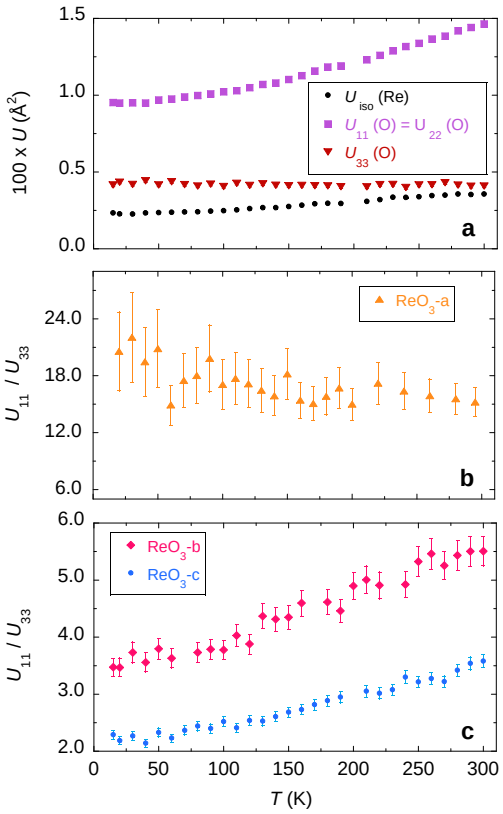

FIG. 4: (a) Temperature evolution of the atomic displacement parameters for ReO_3-c, where U_{iso} represents the rhenium isotropic displacement parameters and U_{11}, U_{22}, U_{33} the oxygen anisotropic displacement parameters. (b) The ratio U_{11}/U_{33} for sample ReO_3-a and (c) the same ratio for samples ReO_3-b and ReO_3-c. U_{11} and U_{22} represent atomic displacement of the oxygen atoms normal to the Re–O–Re bond, while U_{33} to displacement along the bond. Error bars, shown within the symbols in (a), are obtained from the standard uncertainties in the structural refinements.

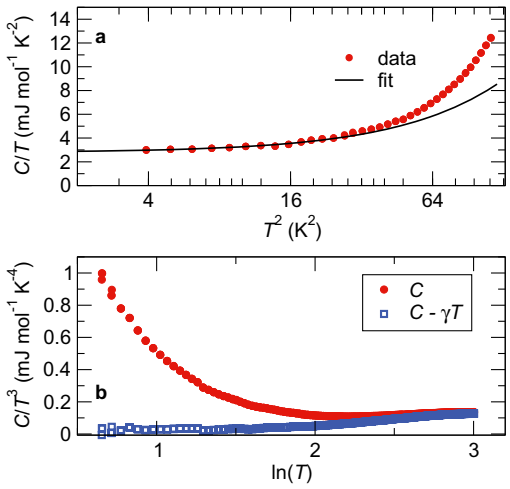

FIG. 5: Specific heat data for a single crystal ReO_3. (a) Data fit below 4 K to the function $C/T = \gamma + \beta T^2$ (where $\Theta^3 = 12/5\pi^4 R/\beta$; R is the gas constant). The fitting allows the Sommerfeld coefficient $\gamma = 3.6\,\mathrm{mJ\,mol^{-1}\,K^{-2}}$ and a Debye temperature of $\Theta = 344\,\mathrm{K}$ to be obtained. (b) Data plotted as C/T^3 *vs.* $\ln T$ in order to reveal any low energy phonon spectral weight. The absence of any peaks indicates a lack of contribution from any Einstein-type modes; the Debye contribution appears as a constant up to Θ and the rise at low $\ln T$ is due to the electronic contribution (γT) of the delocalized electrons.

Although both ZrW_2O_8 and ReO_3 have cubic symmetry, it is interesting to compare how their structures lead do different NTE behavior. The primitive cubic structure of ReO_3 (given the absence of the A cation in its structure and thus an extremal value of the perovskite tolerance factor) is of course the consequence of metallicity: the large volume is maintained by the Fermi pressure of the delocalized d-electrons in the π^* conduction band. Nevertheless, the proximity to a 'buckling transition' is revealed by a pressure-induced collapse of the structure produced by cooperative counter-rotation of the octahedra,[25, 26] in this case very similar to ZrW_2O_8.[27, 28] The linear α obtained for ReO_3 is smaller than that observed in ZrW_2O_8, where $\alpha = -8.7 \times 10^{-6}\ \mathrm{K^{-1}}$. Indeed, the smaller absolute value of the NTE and the smaller temperature range at which it occurs in ReO_3 compared to ZrW_2O_8 is consistent with the much weaker precursor effects in the pressure-induced collapse in the former than in the latter.[28] In turn, the weakness of the fluctuations in ReO_3 is possibly a consequence of it possessing fewer soft degrees of freedom than the more open framework structure of ZrW_2O_8. In addition, the low energy Einstein-type modes observed in ZrW_2O_8 and implicated in that material's NTE behavior,[5, 23] are clearly missing in ReO_3.

The relatively small NTE effect observed in ReO_3 remains, nevertheless, remarkable because it is isotropic and unprecedented for a material with the electronic properties of a simple metal. While classifying an oxide as a simple metal is atypical, the free-electron model works well enough in ReO_3 that it qualifies under the scheme of electrical transport properties (other examples include the Na_xWO_3 bronzes and RuO_2).[29] Most simple metals have a much larger α than that of ReO_3. For example, for copper, α is $16.5 \times 10^{-6}\,\mathrm{K^{-1}}$ at room temperature.[30] Another notable exception is the intermetallic YGaGe, which has such small α that its behavior has been termed zero thermal expansion.[31] Like YGaGe, ReO_3 is also remarkable in that its α above room temperature is as low as in a highly covalent material like diamond where α is $1 \times 10^{-6}\,\mathrm{K^{-1}}$.[21] While ReO_3 does exhibit highly metallic behavior, the strong covalency between the Re d-states and O p-states and its unique framework topology allow for negative thermal expansion, demonstrating the propensity for transition metal oxides to challenge our conventions on bonding and properties in solid materials. Furthermore, ReO_3's relatively simple structure has provided a way to quantify the role of static disorder of the oxygen atoms on interesting behavior such as negative thermal expansion.

IV. ACKNOWLEDGEMENTS

This work has benefited from the use of HIPD at the Lujan Center at Los Alamos Neutron Science Center, funded by DOE Office of Basic Energy Sciences. Los Alamos National Laboratory is operated by Los Alamos National Security LLC under DOE Contract DE-AC52-06NA25396. We would also like to thank J. C. Lashley and A. Lawson from Los Alamos for stimulating discussions and L. L. Daeman, also from Los Alamos, for help with sample preparation. BCM and RS acknowledge the National Science Foundation for support through a Career Award (NSF-DMR-0449354), and for the use of MRSEC facilities (Award nsf-dmr0520415).

[1] C. Kittel, *Introduction to Solid State Physics* (Wiley, 2005), 8th ed.

[2] A. W. Sleight, Inorg. Chem. **37**, 2854 (1998).

[3] T. A. Mary, J. S. O. Evans, Z. Hu, T. Vogt, and

A. W. Sleight, Science **272**, 90 (1996).
[4] J. S. O. Evans, Z. Hu, J. D. Jorgensen, D. N. Argyriou, S. Short, and A. W. Sleight, Science **275**, 61 (1997).
[5] G. Ernst, C. Broholm, G. R. Kowach, and A. P. Ramirez, Nature **396**, 147 (1998).
[6] A. L. Goodwin and C. J. Kepert, Phys. Rev. B **71**, 140301 (2005).
[7] K. W. Chapman, M. Hagen, C. J. Kepert, and P. Manuel, Physica B **385–386**, 60 (2006).
[8] A. Ferretti, D. B. Rogers, and J. B. Goodenough, J. Phys. Chem. Sol. **26**, 2007 (1965).
[9] C. N. King, H. C. Kirsch, and T. H. Geballe, Sol. State Comm. **9**, 907 (1971).
[10] T. Chatterji, P. F. Henry, R. Mitall, and S. L. Chaplot, Phys. Rev. B **78**, 134105 (2008).
[11] A. W. Sleight, Annu. Rev. Mater. Sci. **28**, 29 (1998).
[12] R. Mittal, S. L. Chaplot, S. K. Mishra, and P. P. Bose, Phys. Rev. B **75**, 174303 (2007).
[13] M. P. Attfield and A. W. Sleight, Chem. Comm. **5**, 601 (1998).
[14] P. Lightfoot, D. A. Woodcock, M. J. Maple, L. A. Villaescusa, and P. A. Wright, J. Mater. Chem. **11**, 212 (2001).
[15] N. Matsuno, M. Yoshimi, S. Ohtake, T. Akahane, and N. Tsuda, J. Phys. Soc. Japan **45**, 1542 (1978).
[16] D. Taylor, Br. Ceram. Trans. J. **84**, 9 (1985).
[17] J. Z. Tao and A. W. Sleight, J. Sol. State Chem. **173**, 442 (2003).
[18] H. Nechamkin, A. N. Kurty, and C. F. Hiskey, J. Am. Chem. Soc. **73**, 2829 (1951).
[19] J. Feller, H. Opermann, M. Binnewies, and E. Milke, Z. Naturforsch **53b**, 184 (1998).
[20] A. C. Larson and R. B. Von Dreele, Tech. Rep., Los Alamos National Laboratory Report, LAUR 86-748 (2004).
[21] T.-S. Chang and P. Trucano, J. Appl. Cryst. **11**, 286 (1978).
[22] K. N. Trueblood, H.-B. Bürgi, H. Burzlaff, J. D. Dunitz, C. M. Gramaccioli, H. H. Schulz, U. Shmueli, and S. C. Abrahams, Acta Cryst. **A52**, 770 (1996).
[23] A. P. Ramirez and G. R. Kowach, Phys. Rev. Lett. **80**, 4903 (1998).
[24] A. Junod, T. Jarlborg, and J. Muller, Phys. Rev. B **27**, 1569 (1983).
[25] J.-E. Jørgensen, J. Staun Olsen, and L. Gerward, J. Appl. Cryst. **33**, 279 (2000).
[26] B. Batlogg, R. G. Maines, and M. Greenblatt, Physica B **29**, 3762 (1984).
[27] J. D. Jorgensen, Z. Hu, T. S., D. N. Argyriou, S. Short, J. S. O. Evans, and A. W. Sleight, Phys. Rev. B **59**, 215 (1999).
[28] C. Pantea, A. Migliori, P. B. Littlewood, Y. Zhao, H. Ledbetter, J. C. Lashley, T. Kimura, J. Van Duijn, and G. R. Kowach, Phys. Rev. B **73**, 214118 (2006).
[29] P. A. Cox, *Transition Metal Oxides: An Introduction to their Electronic Structure and Properties* (Oxford University Press, New York, 1992).
[30] D. R. Lide, ed., *CRC Handbook of Chemistry and Physics* (Taylor and Francis Group, Boca Raton, FL, USA, 2008), 88th ed.
[31] J. R. Salvador, F. Guo, T. Hogan, and M. G. Kanatzidis, Nature **425**, 702 (2003).